2010

Identification and characterization of small compound inhibitors of human FATP2

Angel Sandoval
University of Nebraska-Lincoln

Aalap Chokshi
Albany Medical College

Elliot D. Jesch
University of Nebraska-Lincoln

Paul N. Black
University of Nebraska-Lincoln, pblack2@unl.edu

Concetta C. DiRusso
University of Nebraska-Lincoln, cdirusso2@unl.edu

PMCID: PMC2814954

Published in final edited form as:
Biochem Pharmacol. 2010 April 1; 79(7): 990. doi:10.1016/j.bcp.2009.11.008.

Identification and characterization of small compound inhibitors of human FATP2

Angel Sandoval[a], **Aalap Chokshi**[b], **Elliot D. Jesch**[a], **Paul N. Black**[a], and **Concetta C. DiRusso**[a,c,*]

[a] Department of Biochemistry, University of Nebraska-Lincoln, Lincoln, NE 68588-0664

[b] Center for Cardiovascular Sciences, Albany Medical College, Albany, NY 12208

[c] Department of Nutrition and Health Sciences, University of Nebraska-Lincoln, Lincoln, NE 68583-0806

Abstract

Fatty acid transport proteins (FATPs) are bifunctional proteins, which transport long chain fatty acids into cells and activate very long chain fatty acids by esterification with coenzyme A. In an effort to understand the linkage between cellular fatty acid transport and the pathology associated with excessive accumulation of exogenous fatty acids, we targeted FATP-mediated fatty acid transport in a high throughput screen of more than 100,000 small diverse chemical compounds in yeast expressing human FATP2 (hsFATP2). Compounds were selected for their ability to depress the transport of the fluorescent long chain fatty acid analogue, C_1-BODIPY-C_{12}. Among 234 hits identified in the primary screen, 5 compounds, each representative of a structural class, were further characterized in the human Caco-2 and HepG2 cell lines, each of which normally expresses FATP2, and in 3T3-L1 adipocytes, which do not. These compounds were effective in inhibiting uptake with IC_{50}s in the low micromolar range in both Caco-2 and HepG2 cells. Inhibition of transport was highly specific for fatty acids and there were no effects of these compounds on cell viability, trans-epithelial electrical resistance, glucose transport, or long chain acyl-CoA synthetase activity. The compounds were less effective when tested in 3T3-L1 adipocytes suggesting selectivity of inhibition. These results suggest fatty acid transport can be inhibited in a FATP-specific manner without causing cellular toxicity.

Keywords

fatty acid uptake; high throughput screening; FATP; humanized yeast; Caco2; HepG2

1. Introduction

It is becoming increasingly apparent that typical western diets high in fat lead to a plethora of pathophysiological states ranging from obesity and type 2 diabetes to coronary heart disease. One of the hallmarks of these disease states is the accumulation of neutral lipids in the form of triglycerides in non-adipose tissues that normally do not store significant levels of these compounds [1,2]. In these tissues, inflammation and the generation of reactive oxygen species,

*Corresponding author: Tel.: (402) 472-6788; Fax: (402) 472-7842; cdirusso2@unlnotes.unl.edu.

which accompany the increased accumulation of neutral lipids, further contribute to these pathological states. Our laboratory has been investigating the biochemical mechanisms that govern the transport of exogenous fatty acids into cells. While this process includes a diffusional component [3], one mechanism that we have defined is the concomitant transport and esterification of fatty acids by a process referred to as vectorial acylation [4]. This process, while not completely understood in higher eukaryotic systems, is thought to require a fatty acid transport protein (FATP), which functions alone or in conjunction with a long chain acyl-CoA synthetase (Acsl). In a yeast model, compelling evidence has been obtained showing that FATP and Acsl (in yeast Fat1p and Faa1p or Faa4p, respectively) functionally interact at the plasma membrane promoting vectorial acylation [5–7]. When the Fat1p structural gene (FAT1) is deleted, the cells are unable to transport long chain fatty acids and, moreover, are unable to convert exogenous long chain fatty acids to acyl-CoAs, despite having wild type levels of long chain acyl-CoA synthetase activity [6,7]. In yeast cells lacking the two major Acsl structural genes (*FAA1* and *FAA4*), the phenotype is similar, resulting in both the elimination fatty acid transport and the formation of long chain acyl-CoA in response to exogenous challenge [6]. The difference between the *fat1*Δ and *faa1*Δ *faa4*Δ strains is that in the latter there is a 96% reduction in total acyl-CoA synthetase activity.

We have exploited the yeast model system to investigate the biochemical mechanisms underlying the vectorial acylation of exogenous fatty acids. Of particular note has been the use of a *fat1*Δ strain as a host in which to reconstitute the six different mammalian isoforms of FATP [5]. These studies demonstrated that FATP1, FATP2 and FATP4 were fully functional in fatty acid transport, while FATP3, FATP5 and FATP6 were not. We subsequently surveyed the expression of the different FATP isoforms in a number of different mammalian cell types and measured fatty acid transport using the fluorescent long chain fatty acid 4,4-difluoro-5-methyl-4-bora-3a,4a-diaza-s-indacene-3-dodecanoic acid (C_1-BODIPY-C_{12}) [8]. The results of these studies were consistent with the findings from yeast in that cells expressing FATP1, FATP2 or FATP4 were also fatty acid transport proficient.

Using a yeast strain deficient in transport (*fat1*Δ) with depressed acyl-CoA synthetase activity (*faa1*Δ*)* and expressing transport proficient human FATP isoforms, we developed high throughput screening strategies to select for small molecule inhibitors of fatty acid transport using C_1-BODIPY-C_{12} [9,10]. The impetus behind these studies was to identify small molecule inhibitors of fatty acid transport proceeding through a specific FATP isoform so that we could [1] develop additional tools to understand the biochemical mechanisms that govern fatty acid transport into cells, and [2] identify novel compounds of therapeutic value to treat pathological states resulting from, or exacerbated by, fatty acid internalization in non-adipose tissue. In the present study we screened two diverse compound libraries using high throughput strategies developed in our lab; the target in these studies was human FATP2 (hsFATP2) expressed in the yeast *fat1*Δ *faa1*Δ strain. The primary screen of just over 100,000 compounds identified 234 potential hits. On the basis of structural similarities, most could be grouped into five different classes. All 234 compounds were subjected to secondary screens using human Caco-2 cells, which normally express hsFATP2 [8]. A selected subset, representative of the five structural classes, were further characterized in HepG2 cells and 3T3-L1 adipocytes to test inhibition of transport and in Caco2 cells to evaluate impact on additional parameters including barrier function and transport of glucose.

2. Materials and methods

2.1. Materials

Yeast extract, yeast peptone, yeast nitrogen base without amino acids, and dextrose were obtained from Difco (Detroit, MI). Complete amino acid supplement and individual amino acids were from Sigma (St. Louis, MO). Fatty-acid-free bovine serum albumin (FAF BSA)

and other chemical reagents were also from Sigma. The fluorescent long-chain fatty acid analog, 4,4-difluoro-5-methyl-4-bora-3a,4a-diaza-s-indacene-3-dodecanoic acid (C_1-BODIPY-C_{12}) and the fluorescent glucose analog, 2-(*N*-(7-nitrobenz-2-oxa-1,3-diazol-4-yl) amino)-2-deoxyglucose (2-NBDG) were purchased from Molecular Probes/Invitrogen (Eugene, OR, USA). Radioactive fatty acid ([^{3}H] oleate; specific activity, 5 mCi/ml) was obtained from Perkin Elmer (Waltham, MA). BD Biosciences black with clear bottom 384-well and 96-well microplates were used for primary and secondary screenings in yeast. For Caco-2 and HepG2 cells, tissue culture treated 96-well black with clear flat bottom polystyrene collagen coated microplates were obtained from Fisher Scientific (Pittsburgh, PA). Transwell® Permeable Supports used for experiments involving Caco-2 cells were from Corning Life Sciences (Acton, MA).

2.2. Cell culture and reagents

S. cerevisiae strain LS2086 containing deletions within the *FAT1* and *FAA1* genes (*fat1Δfaa1Δ; MATa ura3 52 his3200 ade2-101 lys2-801 leu2-3,112 faa1Δ::HIS3 fat1Δ::G418*) expressing hsFATP2 was used for the primary high throughput screening as detailed previously [9,11]. For most experiments, yeast minimal medium with dextrose (YNBD) containing 0.67% yeast nitrogen base (YNB), 2% dextrose, adenine (20 mg/L), uracil (20 mg/L), and amino acids as required [arginine, tryptophan, methionine, histidine, and tyrosine (20 mg/L); lysine (30 mg/L); and leucine (100 mg/L)] was used. When a rich medium was required, yeast complete media with adenine (YPDA) was used. Growth in liquid culture and on plates was at 30 °C.

The Caco-2 cell line is derived from a human adenocarcinoma and is able to undergo differentiation into polarized epithelial cells that show a brush border phenotype and form well-developed and functional tight junction complexes [12,13]. This cell line is used as an *in vitro* model to predict human intestinal absorption and secretion [14]. Caco-2 cells were maintained in Earl's minimal essential medium (MEM) with 20% FBS in a 95% air 5% CO_2 atmosphere at 37° C, as described [8]. For growth and differentiation, the BD Biosciences Intestinal Epithelium Differentiation Media Pack was used. Cells were plated in basal seeding medium at a density of 2.5×10^5 cells/cm^2 on a collagen-coated black-clear 96-well plate (BD Biosciences). After 72 h in culture, the basal seeding medium was removed and Entero-STIM medium was added to each well. Both media contained mito-serum extender. After another 24 h, cells were serum-starved for one hour in MEM without phenol red prior to performing the C_1-BODIPY-C_{12} uptake assay. HepG2 cells (ATCC, HB-8065) were obtained from the American Type Culture Collection and were cultured according to the supplier's protocols. The cells were seeded in 96-well collagen coated plates at a seeding density of 2.5×10^5 cells/cm^2. 3T3-L1 fibroblasts (ATCC, CL-173) were maintained in modified DMEM and 10% BCS. For differentiation into adipocytes, 3T3-L1 cells were treated with methylisobutylxanthine (0.5mM), dexamethasone (1.0μM), and insulin (1.75μM) in DMEM and 10% FBS for 48 hours as detailed by Student *et al*. [15]. After 48 hour incubation with differentiation medium, cells were treated with DMEM and 10% FBS supplemented with insulin (1.75μM) for 48 hours. Cells were subsequently maintained in DMEM and 10% FBS for an additional 3–6 days until fully differentiated. The number of cells per well in screening trials were determined using the FluoReporter® Blue Fluorometric DNA Quantitation Kit from Invitrogen.

2.3. Library Descriptions and High Throughput Screening

Two chemically diverse compound libraries were screened using our recently devised live-cell HTS method [9]. The NCI Diversity Set Compound Library comprises 1990 chemical core structures representative of a larger compound library of 140,000 compounds (obtained from NCI's Developmental Therapeutics Program (DTP)). The ChemBridge Corporation compound library includes a diverse, drug-like collection of 100,000 compounds.

For primary screening, LS2086 transformed with the hsFATP2 expression vector (pDB126) or transformed with the empty vector (pDB121) along with the GAL4 transcription factor fusion vector, pRS416Gal4-ER-VP16, [16] were pre-grown in YNBD without leucine and uracil (YNBD-leu -ura) as described [9]. The cells were subsequently subcultured to $A_{600\ nm}$ of 0.02 in the same medium containing 10 nM β-estradiol to induce FATP2 expression, grown to mid-log-phase (0.8–1.2 A_{600}), harvested and then resuspended in PBS to a final density of 6×10^7 cells/ml prior to dispensing into a 384-well assay plate (22.5 μl/well; (1.35×10^6 cells)). Wells in the first two rows of each 384-well plate received the vector control cells, and all other wells in the plate received cells expressing hsFATP2. Compounds (2.5 μL) were then added to a final concentration of 40 μM in PBS. After a 2 hr incubation at 30° C, 75 μL of the C_1-BODIPY-C_{12} transport mixture (resulting in final concentrations 1.25 μM C_1-BODIPY-C_{12}, 0.75 μM FAF BSA, 2.1 mM Trypan blue) were added to each well. After 30 min, the cell-associated fluorescence, reflective of fatty acid transport, was measured using a Bio-Tek Synergy HT multidetection microplate reader (Bio-Tek Instruments, Inc. Winooski, VT) using filter sets of 485 nm ± 20 excitation and 528 nm ± 20 emission. The Z′ factor for each plate was calculated using cells expressing hsFATP and vector controls without compound essentially as described [9]. A compound was considered a primary hit when the final fluorescence value was three standard deviation units above or below the positive control fluorescence value obtained for each plate assayed. All compounds that resulted in an increase in cell-associated fluorescence were found to be autofluorescent and were not considered further.

Secondary screens were performed to identify compounds that acted non-specifically as described previously [9]. Compounds were eliminated from further consideration if [1] they were autofluorescent, [2] were able to quench the BODIPY fluorophore, or [3] permeabilized the cells to allow internalization and quenching of trypan blue. Compounds passing each of these secondary screens were subsequently tested for activity primarily using Caco-2 cells as detailed below.

2.4. Compound Evaluation in Caco-2 cells, HepG2 cells and 3T3-L1 Adipocytes

Caco-2 cells were plated in basal seeding medium at a density of 2.5×10^5 cells/cm^2 in collagen-coated 96-well plates, and differentiated as detailed above. HepG2 cells were cultured in EMEM. Differentiated 3T3-L1 adipocytes were maintained in modified DMEM and 10% FBS. After another 24 h, cells were serum-starved for 1 h in MEM without phenol red prior to performing the C_1-BODIPY-C_{12} transport assay [8,17]. In a standard reaction, serum-free MEM was removed from the wells and 50 μL of the test compound in MEM (MEM alone for controls) were added to each well and incubation was continued for 1 h. Then 50 μL of C_1-BODIPY-C_{12} mixture (final concentrations 5 μM C_1-BODIPY-C_{12}; 5 μM FAF BSA; 1.97 mM trypan blue) was added to each well and the uptake was allowed to take place for 15 min. Cell-associated fluorescence was measured as detailed above. The inhibition of fatty acid uptake activity using C_1-BODIPY-C_{12} was assayed using different concentrations of selected compounds ranging from 0.001 μM to 640 μM. Ligand competition curves were fit by nonlinear least-squares regression using one-site competition and dose-response models and Prism software (GraphPad software, Inc., San Diego, CA) in order to determine the compound concentration that reduced C_1-BODIPY-C_{12} fluorescence readout by 50% (IC_{50}). K_i values were calculated from the IC_{50} using the equation of Cheng and Prusoff as detailed in Li *et al* [9] and K_T values published by Sandoval *et al* [8].

To evaluate if inhibition of fatty acid uptake after compound treatment was reversible, cells were seeded in 96-well plates and treated as described above, but after 1 h the media with compound was removed, cells were washed twice with MEM, and fresh media containing

serum was added. Cells were incubated 24 h at 37° C with 5% CO_2 and then fatty acid uptake was measured using the standard C_1-BODIPY-C_{12} transport assay.

2.5. Cytotoxicity Assay in Caco2 Cells

The MTT [3-(4,5-dimethylthiazol-2-yl)-2,5-diphenyltetrazolium bromide] assay was used to determine if compounds of interest were cytotoxic to Caco-2 cells [18]. Cells were cultured and differentiated as detailed above in collagen-coated 96-well plates. Cells were incubated at 37° C, 5% CO_2 for at least one hour and up to 72 h in MEM containing the appropriate dilution of compound. Following this incubation period, the media with compound was removed and 110 μL of MTT reagent (prepared in MEM (final concentration 0.45 mg/mL MTT)) was added. After a 3 h incubation period, the reaction was terminated by the addition of 150 μL stop buffer (0.01 N HCl in 10% SDS). The plates were incubated for 1 h at 37° C to facilitate solubilization of formazan crystals; color development was read at A_{570}.

2.6. Long chain Acyl-CoA Synthetase (Acsl) Activity in Caco-2 Cells After Compound Treatment

Caco-2 cells were grown and differentiated in 60 mm collagen coated dishes (seeding density 2.5×10^5 cells/cm^2). Following growth and differentiation as detailed above, cells were serum starved for 1 h in MEM and then were treated for 1 h with selected compounds at specified final concentrations. The media was subsequently aspirated off and cells washed once with 5 mL PBS, trypsinized using standard procedures and collected by centrifugation. The cell pellet was resuspended in 1 mL STE lysis buffer (10 mM Tris-HCl pH 8.0; 0.1 M NaCl; 1 mM EDTA) and sonicated on ice for 2 min using 3 sec on/off pulses. Samples were clarified by centrifugation (15,000 × *g*, 15 min, 4° C), the supernatant was transferred to a new tube and assayed for oleoyl-CoA synthetase activity (see below); protein concentrations were determined using the Bradford assay using bovine serum albumin as a standard [19]. In parallel experiments, untreated cells were used to prepare the cell extract for Acsl activity measurements where the compound of interest was added directly to the reaction mixture.

Oleoyl-CoA synthetase activity was determined using a reaction mixture containing 200 mM Tris-HCl, pH 7.5, 2.5 mM ATP, 8 mM $MgCl_2$, 2 mM EDTA, 20 mM NaF, 0.01% Triton X-100, 50 μM [^{3}H]-oleic acid ($C_{18:1}$) (dissolved in 10 mg/mL -cyclodextrin), and 0.5 mM coenzyme A. Individual enzyme reactions were initiated by the addition of coenzyme A, incubated at 30° C for 20 min, and terminated by the addition of 2.5 mL of Dole's Reagent (isopropyl alcohol, n-heptane, 1 M H_2SO_4 (40:10:1) [20]. The unesterified fatty acid was removed through organic extraction using n-heptane. Acyl-CoA formed during the reaction remained in the aqueous fraction and was quantified by scintillation counting. Data were expressed as nmol oleoyl CoA formed/min/mg protein.

2.7. Assessment of the Trans Epithelial Electrical Resistance (TEER)

Caco-2 cells were seeded at 2.5×10^5 cells/cm^2 in a 12-well system using Collagen-Coated Transwell®-COL Inserts (Corning Life Sciences). For growth and differentiation, 100 μL of relevant culture medium was added to the upper compartment and 600 μL was added to the lower compartment of each transwell. To assess integrity of the epithelial barrier after compound treatment, the trans epithelial electrical resistance (TEER) test was used. Confluent and fully differentiated cells were starved of serum for 1 h in MEM without phenol red. Subsequently, 100 μL of MEM containing the selected compound or MEM alone were added to the upper compartment and cells were further incubated 1h at 37° C, 5% CO_2. Trans epithelial electrical resistance was then measured using the Millipore Millicell®-ERS system. For each experiment background resistance was determined on a transwell insert without cells.

2.8. Inhibition of Uptake of [^{3}H]-Oleic Acid by Caco-2 cells After Compound Treatment

To assess the inhibition of fatty acid transport using a native fatty acid ligand, 5 μM [^{3}H]-oleate (3.75 μmol/μCi) in 5 μM BSA was added to 60 mm culture dishes containing monolayers of confluent Caco-2 cells differentiated as detailed above that had been pretreated with the compound of interest for 1 h. The transport reaction was initiated by the addition of [^{3}H]-oleate and incubation continued for 3 min. Uptake was stopped by the addition of 6 mL of 100 μM BSA prepared in MEM. The stop cocktail was removed by aspiration and cells rinsed once with a solution 50 μM BSA in MEM to eliminate non-transported fatty acid. Cells were trypsinized, scraped from the culture disk and collected by centrifugation (5 min, 1,500 × *g*). The supernatant was discarded and cells were resuspended in 1 mL of MEM. Triplicate aliquots (20 μL) of the cell suspension were used to measure cell-associated radioactivity, which is reflective of fatty acid transport. A cell aliquot of 40 μL was used to determine the number of viable cells using a bright-line hematocytometer in the presence of 0.4% Trypan blue (w/v). Results were expressed as pmol of fatty acid transported/100,000 cells/3 min. Experiments were repeated at least 3 times.

2.9. Assessment of Glucose Uptake into Caco-2 Cells

To assess the impact of selected compounds upon glucose transport, Caco-2 cells were seeded and differentiated in 96-well collagen coated plates as detailed above and incubated for 1 h with compound diluted in PBS. Glucose transport was assessed by the addition of 50 μL of 2-(*N*-(7-nitrobenz-2-oxa-1,3-diazol-4-yl)amino)-2-deoxyglucose (2-NBDG; final concentration 256 μM) a fluorescent glucose analog [21]. Cells were incubated 30 min at 37° C, 5% CO_2 to allow uptake. The medium was removed by aspiration and cells rinsed once with 100 μL of PBS. Cell-associated fluorescence was measured using a Bio-Tek Synergy HT multidetection microplate reader using 485 ± 20 nm (excitation), 528 ± 20 nm (emission) filter set.

2.10 Data analysis

Values in arbitrary units of the fluorescent signals (AFU) from each HTS plate were acquired using KC4 software in a BioTek Synergy plate reader. These values were exported to Excel (Microsoft Corp., Redmond, WA, USA) spreadsheet templates and the assay quality control Z′ factor was calculated as described [9]. ChemTree software (Golden Helix, Inc., Bozeman, MT, USA) was used for additional statistical analysis and to study structure-activity relationships.

3. Results

3.1. High Throughput Screening in Humanized Yeast

Using yeast cells in which fatty acid transport was dependent upon hsFATP2, we screened two libraries with over 100,000 chemically diverse compounds for inhibition of fatty acid transport using the fluorescent fatty acid analogue C_1-BODIPY-C_{12} [9,10]. Using a selection criterion of a change in fluorescence of 3 standard deviation units from the mean of untreated control cells, this screen identified 234 compounds as potential inhibitors of fatty acid transport. Of these, 8 were eliminated because they quenched the fluorescent signal of C_1-BODIPY-C_{12}; another 10 were eliminated because they apparently disrupted the membrane and increased permeability. The remaining 216 compounds were clustered into structural classes using ChemTree (Golden Helix) and JChem (ChemAxon) analysis software. Compounds that were similar in structure to the atypical antipsychotics identified in a previous screening trial were not considered further since compounds of this type may cause hypertriglyceridemia and other metabolic disturbances upon chronic administration in patients [9]. After structural clustering, most compounds fell into 5 structural classes and a representative of each was chosen for extensive characterization in yeast, 3T3-L1 adipocytes, HepG2 hepatocytes and Caco-2

intestinal epithelial cells. Table 1 lists the names and shows the structures of the selected compounds, as well as the IC_{50} for transport inhibition in Caco-2 and HepG2 cells as well as 3T3-L1 adipocytes. These compounds inhibited fatty acid transport in Caco-2 and HepG2 cells at concentrations in the low micromolar range (Table 1) and resulted in sigmoidal dose response curves (Figure 1). These compounds were not as effective in inhibiting C1-BODIPY-C12 transport in 3T3-L1 adipocytes and resulted in higher IC_{50} values (Table 1,Figure 2), which may be reflective of the different isoforms of FATP being expressed [8]. When tested in Caco-2 cells, none of the selected compounds at 10 times the IC_{50} dosage resulted in cellular toxicity as measured using the MTT assay (Figure 3).

3.2 Reversibility of Selected Compound Action on Fatty Acid Transport

We evaluated whether or not inhibition of fatty acid transport was reversible by incubating Caco-2 cells with compound for one hour, rinsing the cells with MEM and replacing the culture media. After a 24 hour recovery period, fatty acid uptake returned to essentially the pretreatment levels (Table 2). Further characterization was aimed at confirming specific hsFATP mediated fatty acid transport inhibition by these different compounds.

3.3. Inhibition of Fatty acid Transport was Not Due to Nonspecific Effects on the Membrane

We were concerned that treatment with compound might have adverse effects on membrane barrier function by altering, for example, membrane lipid or protein composition. To test if this might be the case, we evaluated the trans epithelial electrical resistance (TEER) in Caco2 cells treated with each of the compounds. None of the compounds caused a significant ($p < 0.05$) change in membrane permeability by this test (Figure 4A).

To evaluate whether other membrane specific processes were disrupted, we measured the transport of the fluorescent glucose analogue 2-NBDG into differentiated Caco-2 cells following incubated with the selected compounds. Glucose transport was not affected by compounds CB-2, CB-5, CB-6 or CB-16 at 20μM, a dosage that maximally inhibits C_1-BODIPY-C_{12} transport. NCI-3 at 50μM reduced 2-NBDG transport slightly (Figure 4B).

3.4 Inhibition of the Transport of Native Fatty Acids

The fluorescent fatty acid analogue C_1-BODIPY-C_{12} is transported and metabolized in a manner similar to the natural fatty acids [9,22]. However, there is always the concern the three fused rings of the BODIPY moiety that do not occur in natural fatty acids might interact with the fatty acid transport apparatus in a manner that is distinct from the native ligands. Therefore we measured fatty acid transport into cells using radioactively labeled oleate ($[^3H]$-$C_{18:1}$). The transport of $[^3H]$-$C_{18:1}$ is linear within the first 5 minutes following initiation of the experiment (data not shown). To test inhibition by our selected fatty acid transport inhibitors, we treated differentiated Caco-2 cells with compounds for 1 hour and measured fatty acid transport using $[^3H]$-$C_{18:1}$ over a 3 minute period. As shown in Figure 5, the transport of oleate, a representative native fatty acid ligand, was significantly inhibited by all 5 compounds ($p \leq 0.01$). These observations corroborate results obtained using C_1-BODIPY-C_{12} to monitor fatty acid transport and inhibition.

3.5. Acsl Activity Remained Unchanged Following Compound Treatment

Upon entry into a cell fatty acids are activated to CoA thioesters by acyl-CoA synthetase (Acsl) in order to enter lipid metabolic pathways. We have shown that in yeast both FATP and Acsl are required for fatty acid transport through the process of vectorial acylation [6,7]. As we selected these small compound inhibitors using a live cell assay, there remained the possibility that Acsl, as opposed to hsFATP2, was the target thereby blocking fatty acid transport. To address whether Acsl was the target of the selected compounds, we pretreated differentiated

Caco-2 cells with compound for 1 hour, removed the compound by rinsing, and then assayed oleoyl CoA synthetase activity in total cell extracts. Oleoyl CoA synthetase activity was not reduced by treatment with CB-5, CB-6, CB-16, or NC-I3 (Figure 6). CB-2, on the other hand at 50μM (10 times the IC_{50}), inhibited activity by about 50%. Similar results were obtained when the compounds were added to cell extracts rather than whole cells (data not shown).

3.6. Comparison of the Activities of Structurally Related Compounds

To test structural features important in inhibition of fatty acid transport by the selected compounds, we next addressed fatty acid transport inhibition of related compounds available from the ChemBridge compound database. The structures can be found in Table 3 and predicted chemical properties in supplemental Table 1. Five compounds similar to CB-2 were evaluated and most were 50 to 100 times less potent than the parent compound (Table 3). One compound, CB-2.3, had an IC_{50} similar to CB2. The only difference between CB-2 and CB-2.3 is fluorine on the R1 phenolic ring as opposed to chlorine. Replacing the sulfur at position R2 with oxygen increases the IC_{50} by 25- to 126-fold. The positions of the methyl ether, hydroxyl and Br on the R3 phenolic ring in CB-2 and CB-2.3 are identical and likely contribute to the ability to block fatty acid transport with comparable efficiency. We tested three related compounds similar to CB-5 and found that the nitrite at position R1 appears to be essential for activity (Table 3B). Only one compound similar to CB-6, CB-6.1, was tested; it was nearly 50-fold less effective (Table 3C). The R groups differ considerably between CB-6 and CB6.1 and thus no conclusions can be made regarding functional groups that disrupt fatty acid transport. We next tested two additional compounds related to CB-16 and found that both had IC_{50}s in the same range as CB-16 (Table 3D). The bromine at position R2 appears to be more critical for maximal activity as opposed to the hydroxyl at position R1.

4. Discussion

Fatty acid transport into cells occurs through a complex process that consists of both diffusional and protein-mediated components. The protein-mediated processes, including those that proceed though selected members of the fatty acid transport protein (FATP) family, are likely to be operational within normal physiological concentrations of fatty acids. In the present work we reconstituted human FATP2 in a yeast strain deficient in its native FATP, Fat1p. In this strain, the fatty acid transport process was fully restored and dependent upon the expression of hsFATP2. Employing this humanized yeast strain and our recently developed HTS method of fatty acid transport using the fluorescent fatty acid analogue C_1-BODIPY-C_{12}, we screened over 100,000 compounds from one commercial (ChemBridge, Corp.) and one public (NCI) compound library for compounds that decreased fatty acid transport. Among the hits identified, 5 compounds, representative of distinct structural classes, were chosen for further characterization since they inhibited transport in the low micromolar concentration ranges in yeast and in two different human cell types that are used as models for intestinal epithelial cells (Caco2) and hepatocytes (HepG2) that also preferentially express FATP2 [8]. The inhibitory properties of each of these 5 compounds was reversible, none disrupted the barrier function of Caco-2 epithelial cells, and each specifically blocked fatty acid transport without disrupting glucose transport or perturbing cell integrity. It was of interest to find that these compounds were less effective in blocking fatty acid transport in 3T3-L1 adipocytes, which express FATP1. Collectively, these studies demonstrate that these five compounds represent lead candidates as mechanistic inhibitors of fatty acid transport mediated through hsFATP2 with potential therapeutic applications.

Previously, we demonstrated that when expressed in yeast defective in fatty acid transport (*fat1*Δ), three FATP isoforms were able to substitute for the yeast FATP, Fat1p. Amongst these was FATP2, the focus of the current study. FATP2 was chosen as the target for these studies

since it is expressed in two human cell lines often used for drug discovery and characterization: HepG2, a line derived from human hepatoma with many characteristics of normal hepatocytes and Caco-2 cells derived from an adenocarcinoma with many characteristics of intestinal epithelial cells [8]. We also addressed whether the selected compounds had the same efficacy when tested in 3T3-L1 adipocytes, which predominantly express FATP1 [8]. FATP2 was first identified as a very long chain acyl-CoA synthetase, called ACSVL1[23]. In fact, all of the FATP family members share amino acid identities and domain architecture similar to the Acsvl family [24]. Our lab demonstrated functional distinctions between long chain fatty acid transport and very long chain activation activities by analysis of an extensive set of *FAT1* alleles mutated in one amino acid [25]. The conclusions made in analyzing these yeast mutants, that activation and transport functions could be distinguished, were further supported by our analysis of six murine FATPs expressed individually in a yeast *fat1*Δ strain. In this case, FATP1, FATP2 and FATP4 could compliment the long chain fatty acid transport deficiency while FATP3, 5 and 6 could not [26]. The current study now provides additional chemical tools with which to further explore contributions of FATP proteins to fatty acid transport.

Our initial screens in yeast provided an effective means to eliminate compounds that decreased cell associated fluorescence through non-specific processes including quenching of the fluorescent fatty acid analogue, permeabilization of the cell membrane, and cytotoxicity. Cytotoxicity was also further evaluated in Caco-2 cells for each of the lead compounds. The compounds selected as part of the final set inhibited fatty acid transport of both the fluorescently labeled fatty acid (C_1-BODIPY-C_{12}) and radioactively labeled fatty acid at low concentrations reflective of the physiological norm. The inhibitors were highly specific for fatty acid transport and did not disrupt other membrane functions; glucose transport was not affected nor was the barrier function of the Caco-2 cells.

One process by which fatty acid transport occurs is through vectorial acylation, which involves specific FATP isoforms that function alone or on concert with a long chain acyl-CoA synthetase (Acsl) [11]. In this coupled transport mechanism the exogenous fatty acid is activated by esterification with coenzyme A concomitant with transport. Fatty acid activation is also required for all subsequent intracellular metabolic transformations. Therefore, in the absence of a cell free binding assay for FATP-fatty acid transport activity, it was important to demonstrate that acyl-CoA synthetase activity was not affected by compound treatment. In the humanized yeast strain, the Acsl providing the activation function coupled to transport is Faa4p. In Caco-2 and HepG2 cells, the specific Acsl required for activation of imported fatty acids has not been defined. We demonstrated that the selected inhibitory compounds did not alter total Acsl activity using two strategies. First, treatment of differentiated Caco-2 cells with the different compounds followed by a washout, did not disrupt oleoyl-CoA synthetase activity in cell extracts; second, Acsl activity was not inhibited when the compounds were directly added to the cell extracts in the reaction mixture. These findings clearly point out that fatty acid transport, likely at the level of FATP2 only, was the target for the selected compounds as long chain acyl-CoA synthetase activity was not decreased. To this end, we conclude that these compounds specifically inhibit fatty acid transport into the cell.

As part of our studies, we addressed whether the expression of a specific FATP isoform changed the efficacy of the selected compounds. As noted above, Caco-2 and HepG2 cells express FATP2 and when treated with the selected compounds gave IC_{50}s in the low micromolar range. When tested in 3T3-L1 adipocytes, the resultant IC_{50}s ranged from 52 to 900 μM. These cells express FATP1 as opposed to FATP2. While there are differences in these cell types beyond the specific FATP isoform expressed, these data indicate that these compounds may be more selective towards FATP2 in the context of fatty acid transport. Further, these data indicate that these compounds may allow more detailed dissection of the individual roles provided by the different FATP isoforms.

A limited number of structurally related compounds were also assessed for ability to inhibit transport. For CB-2 we were able to distinguish a number of features that were essential for activity. The substitution of oxygen for sulfur (R2, Table 3A) as in CB-2.4 and CB2.5 significantly decreased activity (25- to 100-fold). Removal of the bromine at position 3 in CB-2.1 (R3 Table 3A) resulted in a 30-fold drop in activity. In contrast, substitution of the chlorine for fluorine at position 3 in CB-2.3 did not affect activity. This series of compounds and its analogs with a range of potencies in the micromolar range will serve as a reference base from which we will be able to determine structure activity relationships.

The data set for compounds related to CB-5, CB-6 and CB-16 are relatively small and effects on activity more modest. We did determine that the nitrite group on CB-5 (R1, Table 3B) is important for activity as removal decreased activity about 10-fold. Only one compound was available to us related to CB-6 in which the diazepin ring was substituted with a dihydropyrazol-3-ylidene ring and activity was greatly reduced. Substitution or removal of the hydroxide and bromide on CB-16 (R1 and R2, Table 3D) did not change activity.

In the present work we have identified a group of 5 diverse compounds that decrease hsFATP2-mediated fatty acid transport. Each of these compounds has proven to be functional in specifically blocking fatty acid transport without affecting the downstream fatty acid activation. These five compounds are different from the FATP4-specific inhibitors identified by Blackburn, *et al.* using a similar high throughput approach [27]. Those compounds, 4-aryl-3,4-dihydropyrimidin-2(1H)-ones, were structurally distinct from the compounds we have identified. Identification of compounds with unique structural characteristics was not surprising since different FATP orthologues were used in the primary selection by Blackburn and coworkers compared with the screens reported herein.

In conclusion, this study identified and characterized five diverse compounds that inhibit FATP-mediated fatty acid transport in the low micromolar range. Each compound specifically blocks fatty acid transport without impacting other cellular functions and thus is tractable as tools to determine the underlying mechanistic features of the fatty acid transport protein family. An important outcome is that these compounds or structurally related derivatives may provide eventual therapeutic use for disease states in which lipotoxicity is a primary or confounding factor.

Supplementary Material

Refer to Web version on PubMed Central for supplementary material.

Acknowledgments

This work has been supported by grants from the National Institutes of Health (GM56850 and DK07076) and the Charitable Leadership Foundation Medical Technology Acceleration Program to PNB and CCD. Thanks are due to former and present members of the lab for their contributions to this work, including Dr. Hong Li, Ms. Ji-Hong Pan, and Dr. Padmamalini Srinivasan.

Abbreviations

Acsl	acyl-CoA synthetase long chain
FAF BSA	fatty acid free bovine serum albumin
FATP	fatty acid transport protein
C_1-BODIPY-C_{12}	4,4-difluoro-5-methyl-4-bora-3a,4a-diaza-s-indacene-3-dodecanoic
HTS	high throughput screening

MEM	minimal essential media
MTT	3-(4,5-dimethylthiazol-2-yl)-2,5-diphenyltetrazolium bromide
2-NBDG	2-(*N*-(7-nitrobenz-2-oxa-1,3-diazol-4-yl)amino)-2-deoxyglucose
TEER	transepithelial electrical resistance

References

1. Schaffer JE. Lipotoxicity: when tissues overeat. Curr Opin Lipidol 2003;14:281–7. [PubMed: 12840659]
2. Unger RH. Minireview: weapons of lean body mass destruction: the role of ectopic lipids in the metabolic syndrome. Endocrinology 2003;144:5159–65. [PubMed: 12960011]
3. Hamilton JA. Fast flip-flop of cholesterol and fatty acids in membranes: implications for membrane transport proteins. Curr Opin Lipidol 2003;14:263–71. [PubMed: 12840657]
4. Black, PN.; DiRusso, CC. Vecorial acylation: Linking fatty acid transport and activation to metabolic trafficking. In: Goode, J., editor. Fatty acids and lipotoxicity in obesity and diabetes (Novartis Foundation Symposium). London: Wiley; 2007. p. 127-41.
5. DiRusso CC, Li H, Darwis D, Watkins PA, Berger J, Black PN. Comparative biochemical studies of the murine fatty acid transport proteins (FATP) expressed in yeast. J Biol Chem 2005;280:16829–37. [PubMed: 15699031]
6. Faergeman NJ, Black PN, Zhao XD, Knudsen J, DiRusso CC. The Acyl-CoA synthetases encoded within FAA1 and FAA4 in Saccharomyces cerevisiae function as components of the fatty acid transport system linking import, activation, and intracellular Utilization. J Biol Chem 2001;276:37051–9. [PubMed: 11477098]
7. Faergeman NJ, DiRusso CC, Elberger A, Knudsen J, Black PN. Disruption of the Saccharomyces cerevisiae homologue to the murine fatty acid transport protein impairs uptake and growth on long-chain fatty acids. J Biol Chem 1997;272:8531–8. [PubMed: 9079682]
8. Sandoval A, Fraisl P, Arias-Barrau E, Dirusso CC, Singer D, Sealls W, et al. Fatty acid transport and activation and the expression patterns of genes involved in fatty acid trafficking. Arch Biochem Biophys 2008;477:363–71. [PubMed: 18601897]
9. Li H, Black PN, Chokshi A, Sandoval-Alvarez A, Vatsyayan R, Sealls W, et al. High-throughput screening for fatty acid uptake inhibitors in humanized yeast identifies atypical antipsychotic drugs that cause dyslipidemias. J Lipid Res 2008;49:230–44. [PubMed: 17928635]
10. Li H, Black PN, DiRusso CC. A live-cell high-throughput screening assay for identification of fatty acid uptake inhibitors. Anal Biochem 2005;336:11–9. [PubMed: 15582553]
11. Zou Z, Tong F, Faergeman NJ, Borsting C, Black PN, DiRusso CC. Vectorial acylation in Saccharomyces cerevisiae. Fat1p and fatty acyl-CoA synthetase are interacting components of a fatty acid import complex. J Biol Chem 2003;278:16414–22. [PubMed: 12601005]
12. Fogh J, Fogh JM, Orfeo T. One hundred and twenty-seven cultured human tumor cell lines producing tumors in nude mice. J Natl Cancer Inst 1977;59:221–6. [PubMed: 327080]
13. Grasset E, Pinto M, Dussaulx E, Zweibaum A, Desjeux JF. Epithelial properties of human colonic carcinoma cell line Caco-2: electrical parameters. Am J Physiol 1984;247:C260–7. [PubMed: 6476109]
14. Hilgers AR, Conradi RA, Burton PS. Caco-2 cell monolayers as a model for drug transport across the intestinal mucosa. Pharm Res 1990;7:902–10. [PubMed: 2235888]
15. Student AK, Hsu RY, Lane MD. Induction of fatty acid synthetase synthesis in differentiating 3T3-L1 preadipocytes. J Biol Chem 1980;255:4745–50. [PubMed: 7372608]
16. Stafford GA, Morse RH. Chromatin remodeling by transcriptional activation domains in a yeast episome. J Biol Chem 1997;272:11526–34. [PubMed: 9111067]
17. Arias-Barrau, E.; DiRusso, CC.; Black, PN. Methods to monitor fatty acid transport proceeding through vectorial acylation. DA, editor. New York: Humana Press; 2010.

18. Mosmann T. Rapid colorimetric assay for cellular growth and survival: application to proliferation and cytotoxicity assays. J Immunol Methods 1983;65:55–63. [PubMed: 6606682]

19. Bradford MM. A Rapid and Sensitive Method for the Quantitation of Microgram Quantities of Protein Utilizing the Principle of Protein-Dye Binding. Analytical Biochemistry 1976;72:248–54. [PubMed: 942051]

20. Dole VP. A relation between non-esterified fatty acids in plasma and the metabolism of glucose. Journal of Clinical Investigations 1956;35:150–4.

21. Yamada K, Nakata M, Horimoto N, Saito M, Matsuoka H, Inagaki N. Measurement of glucose uptake and intracellular calcium concentration in single, living pancreatic beta-cells. J Biol Chem 2000;275:22278–83. [PubMed: 10748091]

22. Sabah J, McConkey E, Welti R, Albin K, Takemoto LJ. Role of albumin as a fatty acid carrier for biosynthesis of lens lipids. Exp Eye Res 2005;80:31–6. [PubMed: 15652523]

23. Jia Z, Pei Z, Maiguel D, Toomer CJ, Watkins PA. The Fatty Acid Transport Protein (FATP) Family: Very Long Chain Acyl-CoA Synthetases or Solute Carriers? J Mol Neurosci 2007;33:25–31. [PubMed: 17901542]

24. Watkins PA, Maiguel D, Jia Z, Pevsner J. Evidence for 26 distinct acyl-CoA synthetase genes in the human genome. J Lipid Res. 2007

25. Zou Z, DiRusso CC, Ctrnacta V, Black PN. Fatty acid transport in Saccharomyces cerevisiae. Directed mutagenesis of FAT1 distinguishes the biochemical activities associated with Fat1p. J Biol Chem 2002;277:31062–71. [PubMed: 12052836]

26. DiRusso CC, Connell EJ, Faergeman NJ, Knudsen J, Hansen JK, Black PN. Murine FATP alleviates growth and biochemical deficiencies of yeast fat1 strains. Eur J Biochem 2000;267:4422–33. [PubMed: 10880966]

27. Blackburn C, Guan B, Brown J, Cullis C, Condon SM, Jenkins TJ, et al. Identification and characterization of 4-aryl-3,4-dihydropyrimidin-2(1H)-ones as inhibitors of the fatty acid transporter FATP4. Bioorg Med Chem Lett 2006;16:3504–9. [PubMed: 16644217]

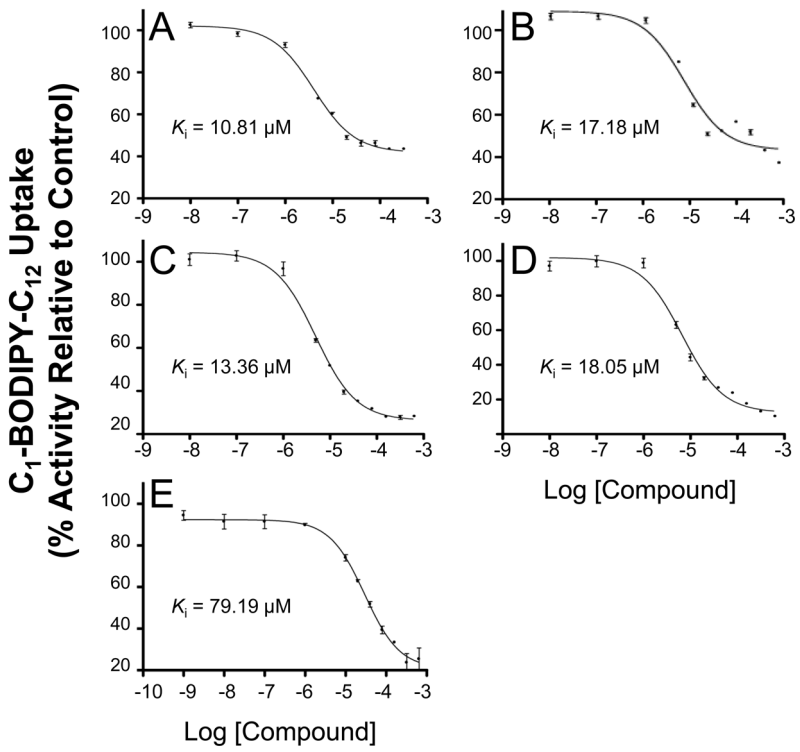

Fig. 1.

Titration of selected compounds yields sigmoidal dose-response curves for the inhibition of C_1-BODIPY-C_{12} uptake into Caco-2 cells. Curves were fit using dose-response nonlinear least-squares regression models in Prism software. (A) compound CB-2; (B) compound CB-5; (C) compound CB-6; (D) compound CB-16; and (E) compound NCI-3. Values are presented as means ± SE for 3–4 experiments assayed in triplicate.

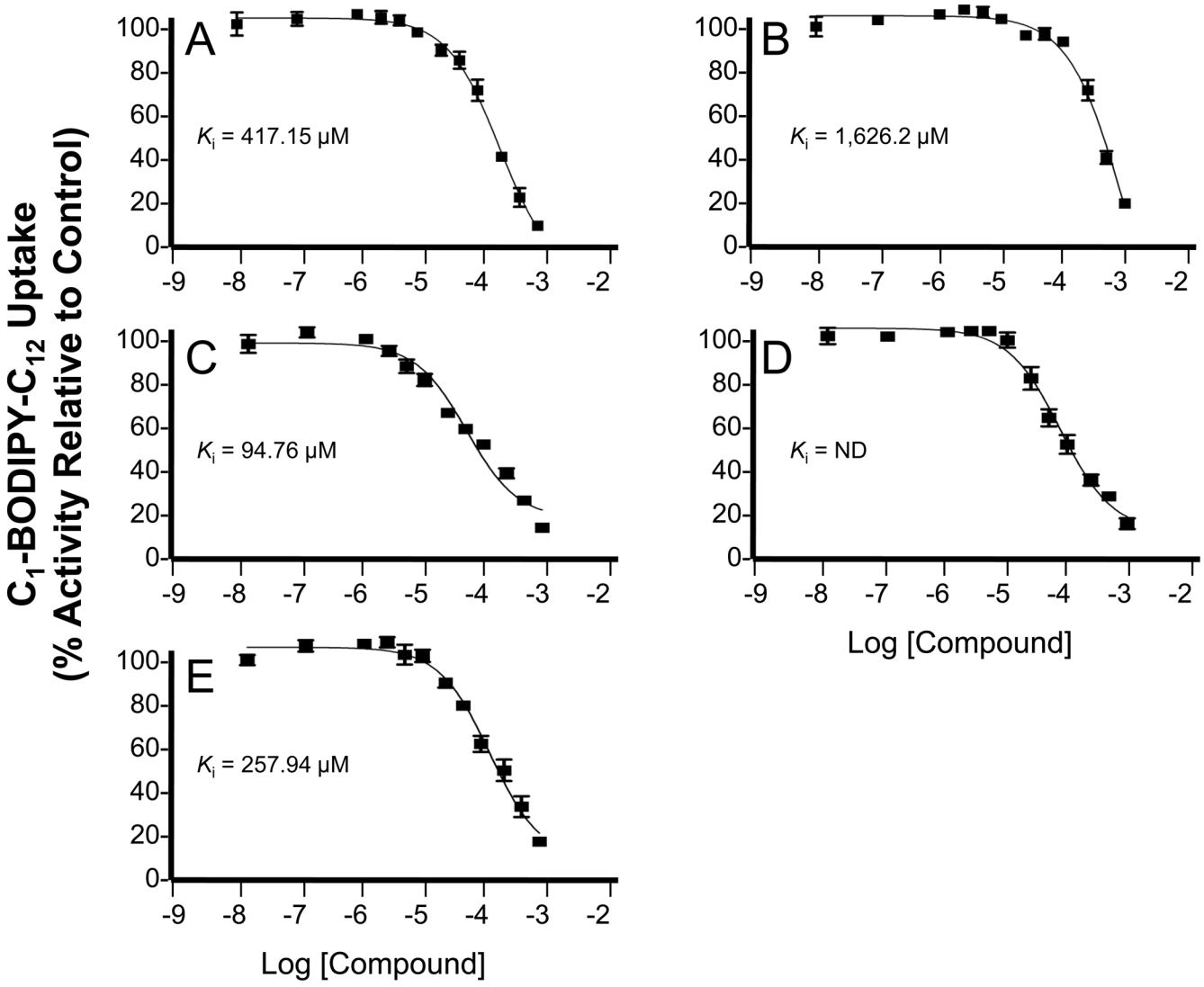

Fig. 2.

Dose-response curves for the inhibition of C_1-BODIPY-C_{12} uptake into 3T3-L1 adipocytes. Curves were fit using dose-response nonlinear least-squares regression models in Prism software. (A) compound CB-2; (B) compound CB-5; (C) compound CB-6; (D) compound CB-16.1; and (E) compound NCI-3. Values are presented as means ± SE for 4 experiments assayed in triplicate.

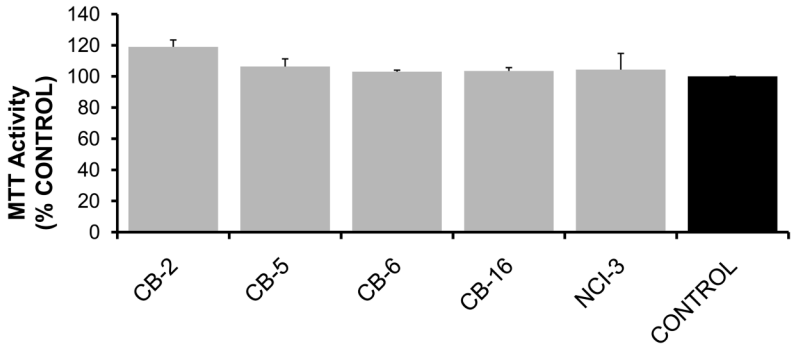

Fig. 3.

The selected compounds are not toxic to cells. Caco-2 cells were treated with CB-2, CB-5, CB-6 or CB-16 at 50 μM, or NCI-3 at 100 μM for 24 h then the MTT assay was performed to assess mitochondrial function, an indicator of cellular toxicity. Bar height indicates the mean value ± standard deviation for 2 experiments assayed in triplicate.

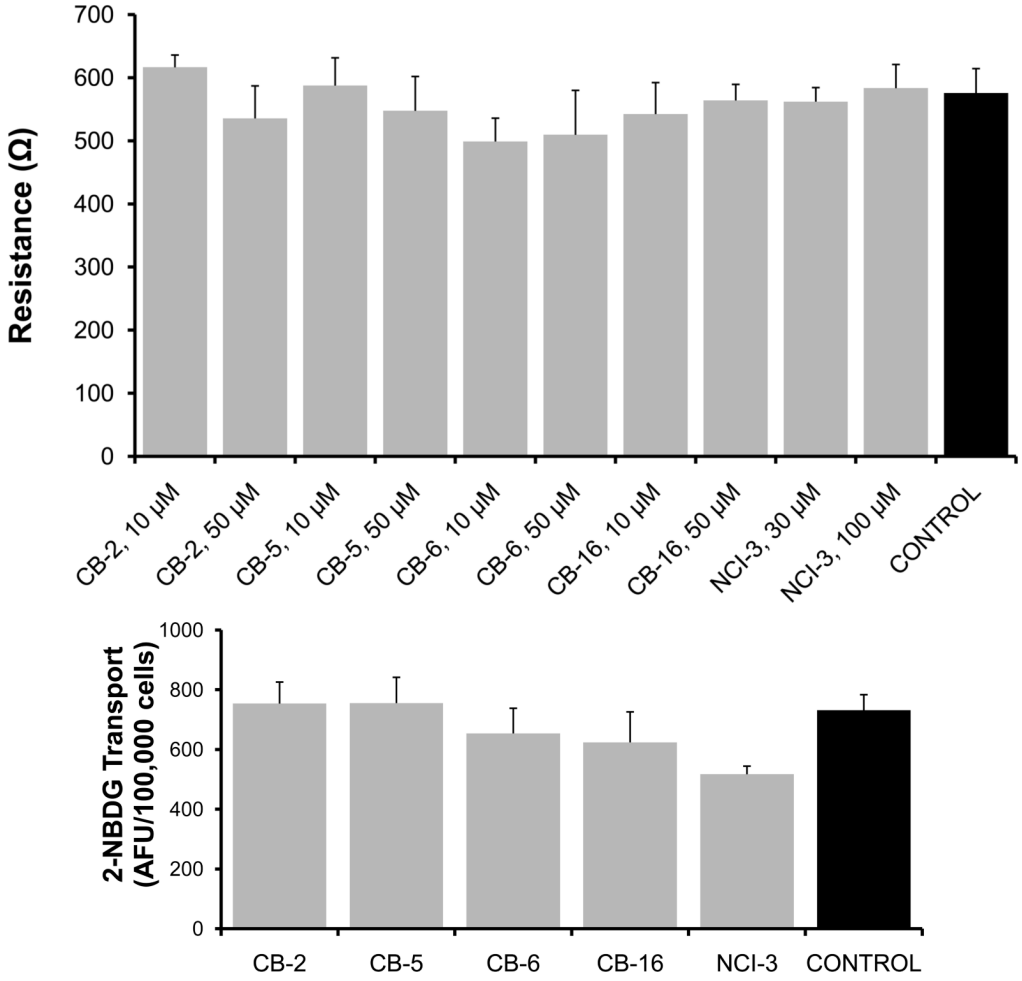

Fig. 4.

Evaluation of barrier and membrane function of Caco-2 cells after compound treatment. (A) Trans-epithelial electrical resistance (TEER) was measured in fully differentiated Caco-2 cells after one hour treatment with two different concentrations of selected compounds as shown. Caco-2 cells were seeded and differentiated in Collagen-Coated Transwell®-COL Inserts. TEER was measured using a Millipore Millicell®-ERS device. (B) Transport of the glucose analogue 2-NBDG was measured in Caco-2 cells seeded and differentiated in 96-well plates. Final concentrations of compounds were 20 μM for compounds CB-2, CB-5, CB-6 and CB-16; and 50 μM for compound NCI-3. Bar height indicates mean values ± standard deviation for 3–5 independent experiments assayed in duplicate (A) and triplicate (B) respectively.

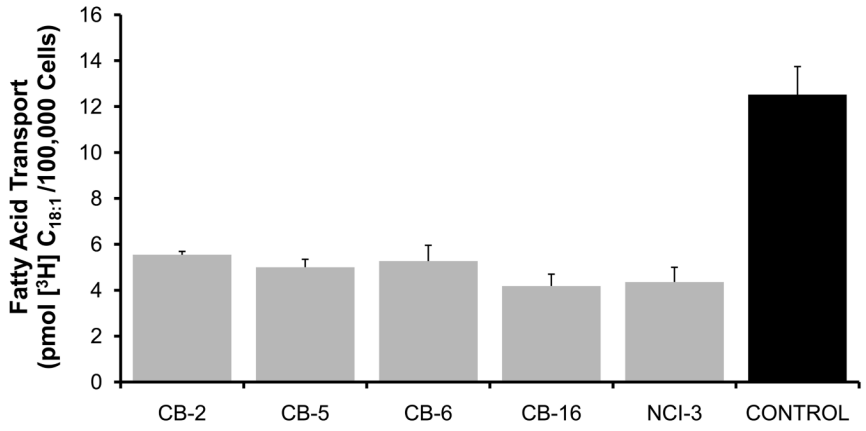

Fig. 5.

Inhibition of uptake of [^{3}H]$C_{18:1}$ into Caco-2 cells. Caco-2 cells were preincubated for one hour with selected compounds (final concentrations were 20 μM for compounds CB-2, CB-5, CB-6 and CB-16; and 50 μM for compound NCI-3) followed by the addition of [^{3}H]$C_{18:1}$ for 3 minutes as detailed in the text. Bar height indicates the mean values ± standard deviation for 3–5 independent experiments.

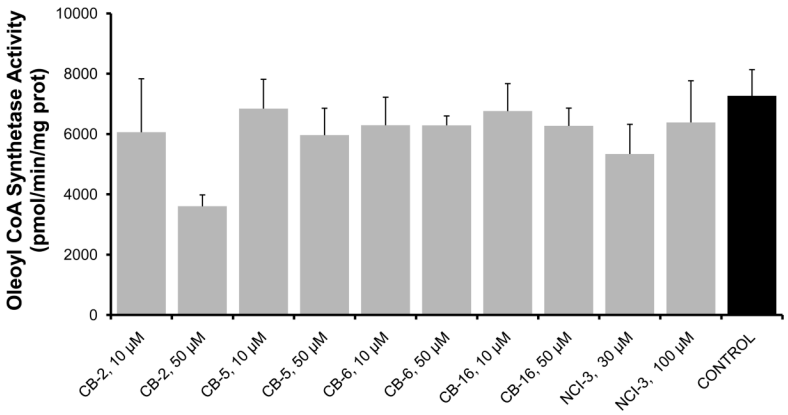

Fig. 6.

Assessment of oleoyl ($C_{18:1}$)-CoA synthetase activity after compound treatment. Cells were treated for 1 h at the indicated final concentration, then cell extracts were prepared and Acsl activity measured. Bar height indicates mean values ± standard deviation for 3–5 independent experiments assayed in duplicate.

TABLE 1

and activity of inhibitory compounds

d Code	Compound ID	Chemical Structure [a]	Caco-2 IC_{50} (μM)[b]	HepG2 IC_{50} (μM)	3T3-L1 Adipocytes IC50 (μM)
	5584680	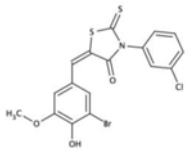	3.99 ± 0.32	7.55 ± 1.23	231.1 ± 33.5
	5674124	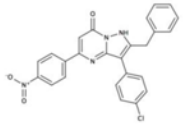	6.34 ± 0.93	10.15 ± 1.26	900.9 ± 204.6
	6022153	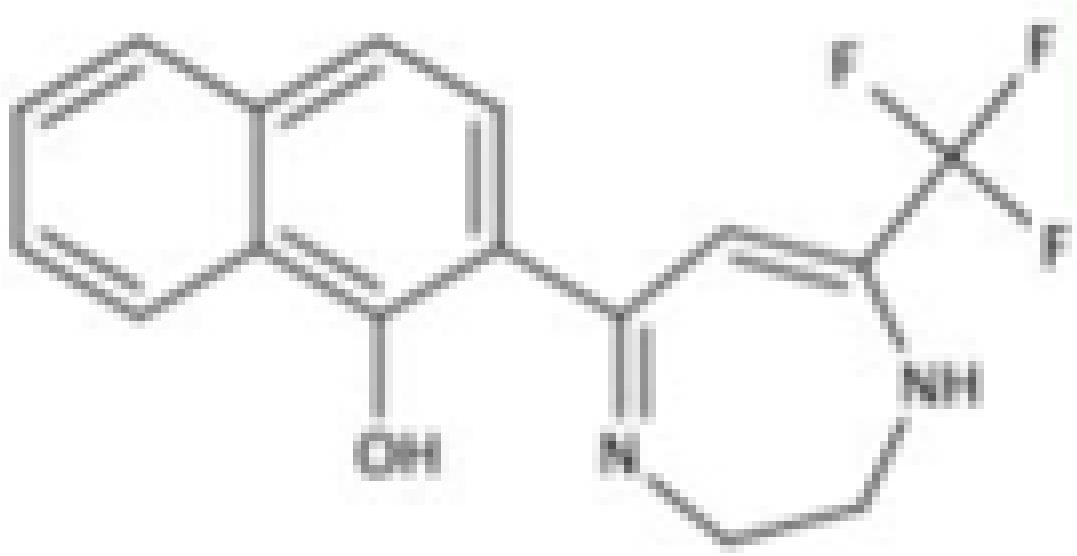	4.93 ± 0.40	6.72 ±0.81	52.5 ± 6.7

Biochem Pharmacol. Author manuscript; available in PMC 2011 April 1.

Internal Code	Compound ID	Chemical Structure [a]	Caco-2 IC_{50} (μM)[b]	HepG2 IC_{50} (μM)	3T3-L1 Adipocytes IC50 (μM)
	5675786		6.66 ± 0.64	ND	ND

d Code	Compound ID	Chemical Structure [a]	Caco-2 IC_{50} (μM)[b]	HepG2 IC_{50} (μM)	3T3-L1 Adipocytes IC50 (μM)
	372127	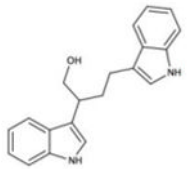	29.22 ± 3.64	84.12 ± 14.12	142.9 ± 22.4

lames: CB2, (5E)-5-[(3-bromo-4-hydroxy-5-methoxyphenyl)methylene]-3-(3-chlorophenyl)-2-thioxothiazolidin-4-one; CB5, 2-benzyl-3-(4-chlorophenyl)-5-(4-nitrophenyl)-1H-pyrazolo[5,1-b]
ne; CB6, 2-[7-(trifluoromethyl)-2,3-dihydro-1H-1,4-diazepin-5-yl]naphthalen-1-ol; CB16, 5′-bromo-5-(6-oxocyclohexa-2,4-dien-1-ylidene)spiro[1,3,4-thiadiazolidine-2,3′-1H-indole]-2′-one;
bis(1H-indol-3-yl)butan-1-ol

e averages of 3 experiments plus and minus the standard error of the mean. ND, not determined

TABLE 2

Compound inhibition is reversible

Compound[a]	% Transport Standard Assay[b]	% Transport after 24 Hour Recovery
Control (no compound)	100	100
CB-2	46 ± 3	93 ±13
CB-5	54 ± 1	88 ±18
CB-6	35 ± 1	74 ± 12
CB-16	27 ± 1	99 ± 16
NCI 3	52 ± 2	99 ±16

[a] All compounds added at f.c. 40 μM to Caco-2 cells

[b] Numbers are the mean of 3–5 experiments ± the standard deviation

TABLE 3

Analysis of compounds structurally related to CB-2, CB-5, CB-6 and CB-16 in Caco-2 cells

A. CB-2

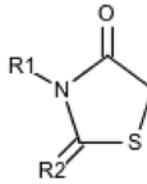

Compound	R1	R2
CB-2	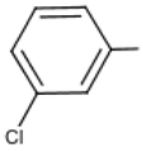	S

A. CB-2

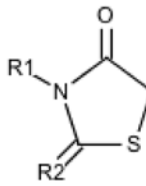

Compound	R1	R2
CB-2.1	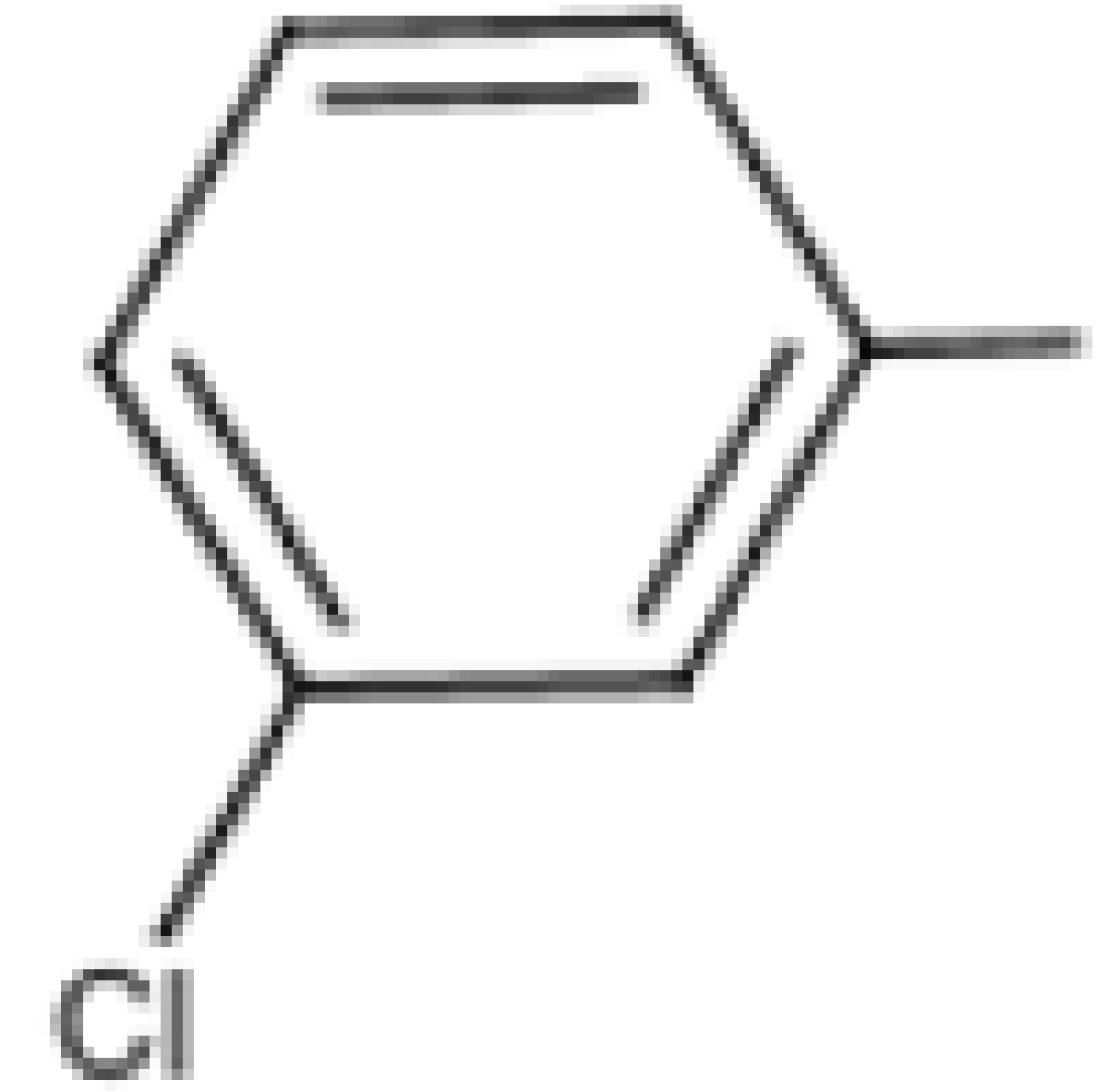	S

A. CB-2

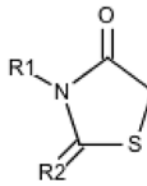

Compound	R1	R2
CB-2.2	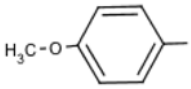	S
CB-2.3	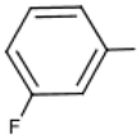	S
CB-2.4	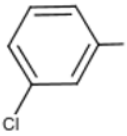	O

A. CB-2

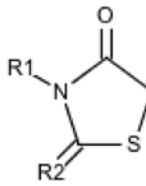

Compound	R1	R2
CB-2.5	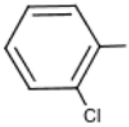	O

B. CB-5

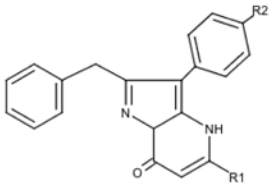

Compound	R1	R2	IC_{50} (μM)
CB-5	NO_2	Cl	6.34 ± 0.93

B. CB-5

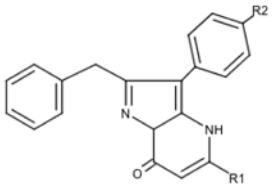

Compound	R1	R2	IC_{50} (μM)
CB-5.1	NO_2	OCH_3	17.3 ± 3.01
CB-5.2	NO_2	H	16.4 ± 2.22
CB-5.3	H	CL	76.9 ± 15.7

C. CB-6

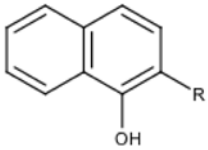

Compound	R	IC_{5}
CB-6	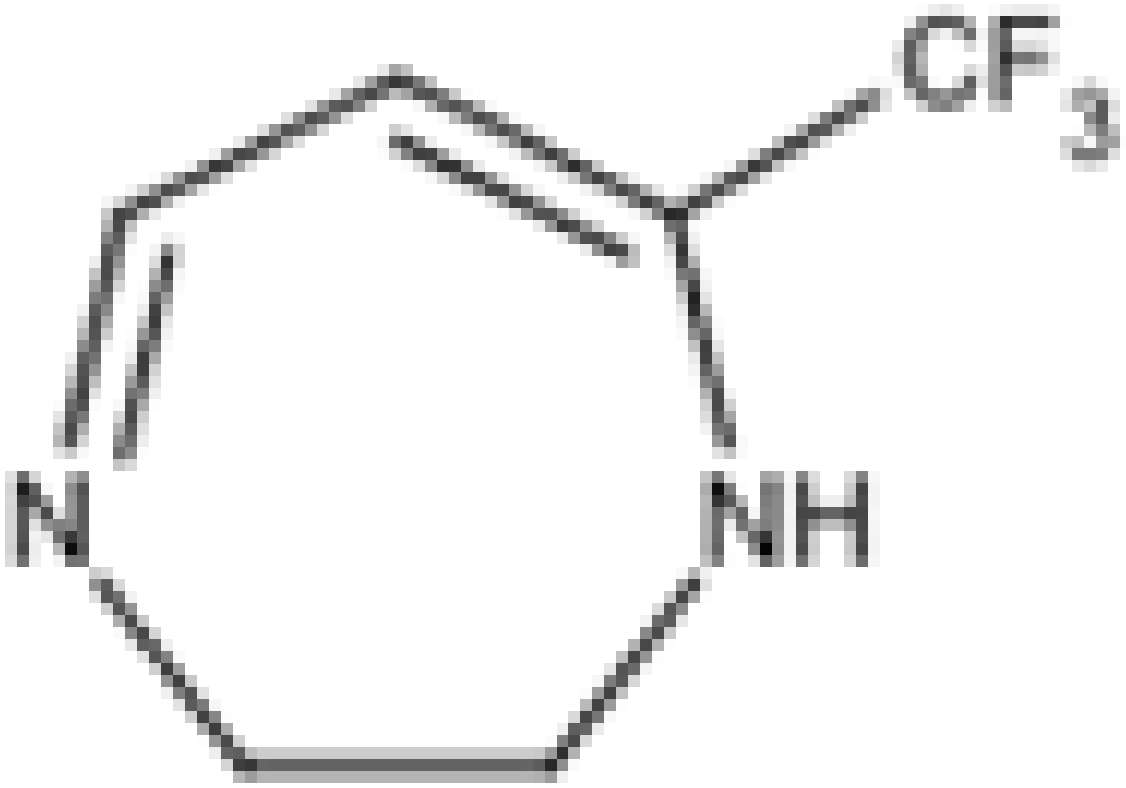	4.93

C. CB-6

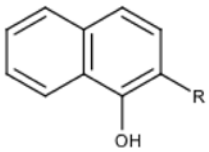

Compound	R	IC_{50}
CB-6.1	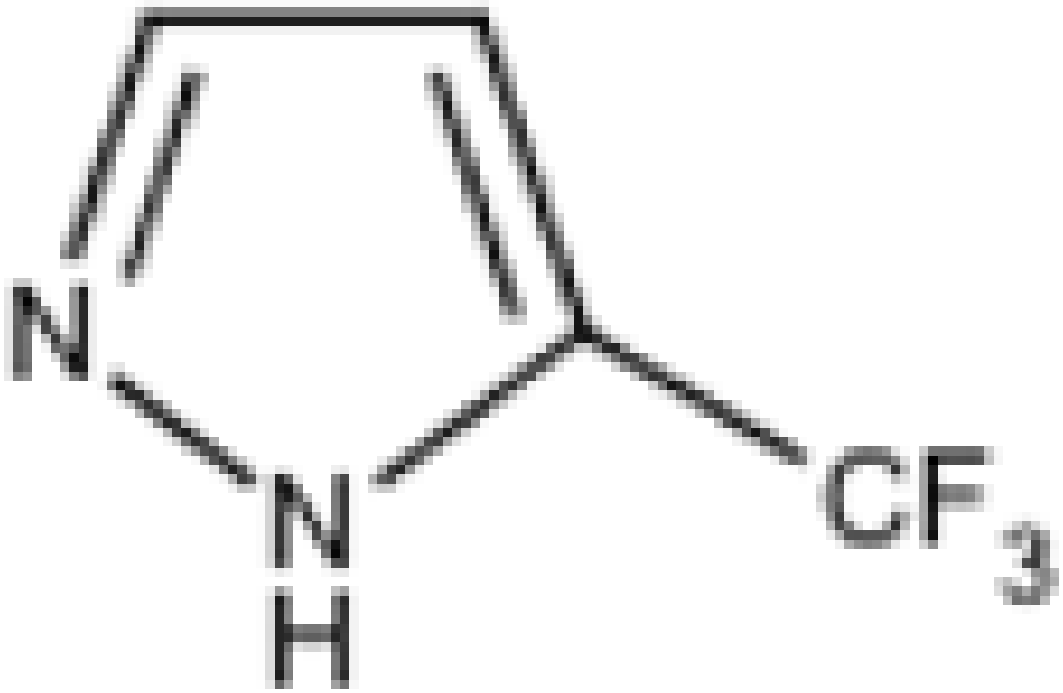	241

D. CB-16

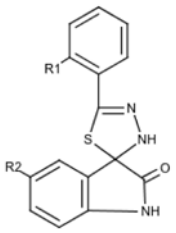

Compound	R1	R2	IC_{50} (μM)
CB-16	OH	Br	6.66 ± 0.64
CB-16.1	OH	H	11.9 ± 1.43
CB-16.2	H	Br	4.84 ± 0.69